

Comparison of simulation methods applied to steel bridge reliability evaluations

Ruoqi Wang

PhD student, Division of Structural Engineering and Bridges, KTH Royal Institute of Technology, Stockholm, Sweden

John Leander

Associate Professor, Division of Structural Engineering and Bridges, KTH Royal Institute of Technology, Stockholm, Sweden

Raid Karoumi

Professor, Division of Structural Engineering and Bridges, KTH Royal Institute of Technology, Stockholm, Sweden

ABSTRACT: Steel bridges are in general subjected to fatigue deterioration and the structural reliability of bridges will thus reduce over time. There are multiple simulation-based procedures available to perform structural probabilistic studies with several classes of uncertainty taken into account. Since the crack propagation is highly nonlinear and the limit state function (LSF) is multi-dimensional, it imposes specific demands on the simulation methods. Monte Carlo simulation (MCS) has been widely applied in various of fields, however, it requires a great amount of samples and long computation time to reach a high level of accuracy. A more advanced method, Subset Simulation (SS), compensates this shortage. It calculates the product of conditional probabilities of several chosen intermediate failure events. In this paper, the performance of each method was evaluated and compared against fatigue deterioration for a selected bridge detail. A probabilistic model was defined and both prior and updated reliability estimation were performed. The results showed that SS is a good option to deal with fatigue problem with high nonlinearity and multi-dimensional LSF, and shows outstanding time efficiency compared to MCS to reach a comparable accuracy.

1. INTRODUCTION

Fatigue is among the most critical forms of deterioration damage that occurs to steel bridges. It's usually causing a decline of the safety level over time due to repeated or varying loading. The initiation and propagation of a fatigue crack is a strongly nonlinear phenomenon due to the exponential relation between crack growth and stress range, varying crack growth rates, and threshold levels. The limit state function (LSF) is always a multi-dimensional problem considering different levels of uncertainty. Both aspects impose more demands on the simulation methods. In this paper, Monte Carlo Simu-

lation (MCS) and the Subset Simulation (SS) are selected, presented and compared.

MCS is a straightforward and robust method to perform the reliability assessment. However, when the probability of failure is a small number, a great number of samples are usually required to reach a high level of accuracy (Mooney (1997)), which in turn require time-consuming calculation. The efficiency of MCS can be enhanced by importance sampling. But it was discovered by Au and Beck (2003) that when many stochastic variables considered in the problem, the importance sampling fails to describe the importance region which will lead

to an increase in the variance of the result. A more advanced method as Subset Simulation could compensate this shortage.

SS is an adaptive Monte Carlo method particularly suitable for handling problems involving a large number of random variables, both robust to applications and competitive in terms of efficiency (Au and Wang (2014)). Due to its special calculation routine, it takes less time than MCS for a comparable accuracy. All variables are suggested to be transferred to the standard normal space, especially when the correlations between variables are considered. Currently, SS are mainly applied to the problems considering normal distributed stochastic variables (Papaioannou et al. (2015), Song et al. (2009)) or with a relatively linear LSF (Wang and Li (2017)).

The Rautasjokk Bridge, a railway steel bridge in the northern Sweden, was selected as a case study. The reliabilities for some components in the bridge were assessed using measured data from a monitoring campaign. Both simulation methods were applied to solve a complex and nonlinear LSF with several lognormal distributed variables considered.



Figure 1: A photo of the Rautasjokk Bridge

2. METHODOLOGY

2.1. Probabilistic model

To avoid unduly conservatism by a deterministic approach, and due to the various levels of uncertainty involved in the problem considering fatigue, a probabilistic model was established. It is based on linear elastic fracture mechanics (LEFM) and Paris law for crack growth.

Paris (1961) proposed a crack-growth model, which describes the relationship between cyclic

crack growth and the stress intensity factor range:

$$\frac{da}{dN_r} = AK_r^m \quad (1)$$

where a is the crack size, N_r is the number of stress cycles, A and m are fatigue growth parameters. K_r is the stress intensity factor range, depending on the stress range S , the crack size and the geometry of the considered detail. K_r is expressed as:

$$K_r(a) = S\sqrt{\pi a}Y(a)M_k(a) \quad (2)$$

where $Y(a)$ is a geometry correction factor considering the geometry of the unwelded component, and $M_k(a)$ is a stress magnification factor due to the weld geometry (Hobbacher (1992)).

For the analyses presented in this paper, a bi-linear crack growth rate relation have been adopted as suggested in BS 7910:2013 (BSI (2013)). It is expressed as:

$$\frac{da}{dN_r} = \begin{cases} 0 & K_r < K_{th} \\ A_a K_r^{m_a} & K_{th} \leq K_r < K_{ab} \\ A_b K_r^{m_b} & K_r \geq K_{ab} \end{cases} \quad (3)$$

where K_{th} is the crack growth threshold below which K_r causes no crack growth. The transition point K_{ab} is calculated as:

$$K_{ab} = \left(\frac{A_a}{A_b} \right)^{1/(m_b - m_a)} \quad (4)$$

The bi-linear crack growth law in Eq. (3) is plotted in Figure 2 with mean and 95% confidence interval. The characteristic values of each stochastic variable considered can be found in Table 1.

Based on the crack growth law, the number of cycles to reach a critical crack depth is calculated as:

$$N_c(\mathbf{x}) = \int_{a_0}^{a_{cr}} \left(\frac{da}{dN_r} \right)^{-1} da \quad (5)$$

where a_0 is the initial crack size and a_{cr} is the critical crack size. The vector \mathbf{x} contains the stochastic variables considered in the probabilistic model.

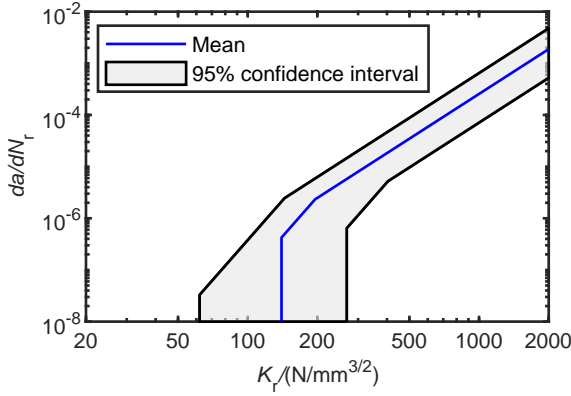


Figure 2: Bi-linear crack growth law

2.2. Reliability assessment

A general LSF considering fatigue is formulated on the number of cycles as:

$$g(\mathbf{x}, t) = N_c(\mathbf{x}) - N_s(t) \quad (6)$$

where $N_c(\mathbf{x})$ is described by Eq. (5) and $N_s(t)$ is the number of cycles at the studied point in time.

Reliability analysis is concerned with the evaluation of the probability of failure, defined as:

$$P_f = P(g(\mathbf{x}) \leq 0) = \int_{g(\mathbf{x}) \leq 0} f_{\mathbf{x}}(\mathbf{x}) d\mathbf{x} \quad (7)$$

where $f_{\mathbf{x}}(\mathbf{x})$ is the joint probability density function (PDF) of all stochastic variables contained in \mathbf{x} , and $g(\mathbf{x}) \leq 0$ represents the region of failure in \mathbf{X} -space.

The parameter β , often called the ‘‘Hasofer–Lind reliability index’’, is a convenient measure of reliability. It is related to the probability of failure as:

$$\beta = -\Phi^{-1}(P_f) \quad (8)$$

where $\Phi^{-1}()$ is the inverse of the standardized normal distribution function. In this paper, $\beta = 3.1$ is selected as the target reliability level according to the suggestion in ISO 13822 (2010), corresponding to a probability of failure as 10^{-3} .

2.3. Reliability updating

2.3.1. Detection event

If the theoretical assessment is based on a measured indication of damage, the prior estimation of the reliability can be updated considering results

from inspection. The detection event can be established as:

$$H_D(\mathbf{x}) = a(\mathbf{x}, N_{ri}) - a_d \quad (9)$$

where $a(\mathbf{x}, N_{ri})$ is the estimated crack size at cycle N_{ri} , and a_d is the lower bound limit of detectable crack size described by a probability of detection (PoD) curve. Then the estimated probability of failure can be updated assuming no crack is detected ($H_D \leq 0$) as:

$$P_f^{\text{up}} = P[g(\mathbf{x}) \leq 0 \mid H_D(\mathbf{x}) \leq 0] \quad (10)$$

2.3.2. PoD curve

The accuracy of the inspection is dependent on the PoD curve. Here the recommended curve issued by DNV GL (2015) is adopted since it has been widely used in Offshore Technology, and proved to be robust under application. It’s expressed as:

$$PoD(x) = 1 - \frac{1}{1 + \left(\frac{x}{X_0}\right)^{X_1}} \quad (11)$$

In this paper, visual inspection is selected due to its simplicity and low-cost in practice. For visual inspection, x indicates the lower bound of detectable crack length and the values for X_0 and X_1 are 15.78 and 1.079 respectively.

2.4. Simulation methods

2.4.1. Monte Carlo Simulation

The MCS method was firstly developed and applied in the 1940s, and has become more feasible in various fields with the increasing availability of fast computers. It is an intuitive approach that solves a problem by simulating directly the physical process. Its procedure can be found in Mooney (1997).

2.4.2. Subset Simulation

The SS method was proposed by Au and Beck (2001). It has been widely applied as a strong simulation engine, especially for rare events calculation. The number of samples N and conditional probability p_0 for each subset iteration are the only input for the SS routine, in addition to the LSF and stochastic variables.

In order to make SS more applicable, it is suggested to transform all the stochastic variables to the standard normal probability space \mathbf{U} through an one-to-one mapping $\mathbf{U} = \mathbf{T}(\mathbf{X})$ (Hohenbichler and Rackwitz (1981)), especially when the correlations between variables are considered. Then Eq. (7) is transformed into:

$$P_f = \int_{G(\mathbf{u}) \leq 0} f_{\mathbf{u}}(\mathbf{u}) d\mathbf{u} \quad (12)$$

where $f_{\mathbf{u}}(\mathbf{u})$ is the standard normal joint PDF and $G(\mathbf{u}) = g(\mathbf{T}^{-1}(\mathbf{u}))$ is the LSF in the \mathbf{U} -space.

By expressing the event F as an intersection of M intermediate events, P_f is estimated as a product of conditional probabilities:

$$P_f = P\left(\bigcap_{j=1}^M F_j\right) = \prod_{j=1}^M P(F_j | F_{j-1}) \quad (13)$$

where F_0 is a certain event. The intermediate events are defined as $F_j = \{G(\mathbf{u}) < b_j\}$, where the values of b_j are p_0 -percentile of the calculated values of $G(\mathbf{u})$. The iteration stops only when $b_j \leq 0$. Then the probability of failure is obtained as:

$$P_f = p_0^{j-1} \frac{N_f}{N} \quad (14)$$

where N_f is the number of failure points in the last iteration.

An adaptive conditional Markov Chain Monte Carlo sampling method from Papaioannou et al. (2015) was referred and applied for sample generation in this paper.

3. CASE STUDY

3.1. The Rautasjokk Bridge

The Rautasjokk Bridge is located along the iron ore railway line in Northern Sweden, between Kiruna and Abisko. A photo of the bridge is shown in Figure 1. The load carrying structure consists of two simply supported parallel steel trusses, with a span length of 33 meters. The single track is carried by stringer beams, which in turn spans between crossbeams. The Rautasjokk Bridge is selected as a case study because it's representative for many similar railway bridges in Sweden and globally. And it also showed strong indications of an exhausted fatigue life due to high load level from iron ore trains (Häggström (2015)).

3.2. Monitoring and stress data

Monitoring the stress is always highlighted as a method to increase the accuracy of the estimation of bridge fatigue life (Liu et al. (2010), Leander et al. (2010), Guo and Chen (2013)).

The monitoring campaign of the Rautasjokk Bridge consists of six uni-axial strain gauges. Their positions are shown in Figure 3. Gauges 101 and 102 were mounted on the vertical flange edges of the stringer beam. Gauge 103 was mounted on the top of the flange close to the end of the cover plate. Gauge 104 was mounted to the bottom edge of the first diagonal of the main truss. Lastly, gauges 105 and 106 were mounted to the top of the crossbeam close to the edges. The monitoring lasted from 25 October 2017 to 30 April 2018, with a total of 4029 train passages registered during this period.

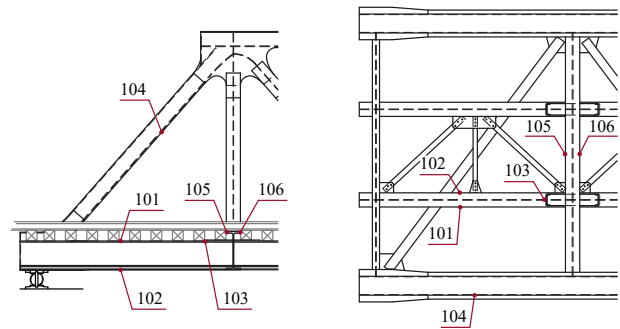


Figure 3: The mounting positions of strain gauges

4. RESULTS

The reliability analyses were performed considering the probabilistic model described in Section 2.1. The stochastic variables considered are listed in Table 1. $C_S = C_{SIF} = 1$ represent model uncertainties for the stress range and the stress intensity factor range respectively. The other variables are selected as suggested in the JCSS (2011) Probabilistic Model.

A preliminary assessment has been performed by using the monitoring data. The result is consistent with previous work from Häggström (2015), showing that gauges 101 and 102 located close to the gusset plate on the stringer beam have the most critical reliability status. Figure 4 shows the dimension of the gusset plate, which is prone to failure.

Table 1: Stochastic variables. LN \sim Lognormal distribution, DET \sim Deterministic value. Crack growth - [mm/cycle], stress intensity - [MPa $\sqrt{\text{mm}}$].

| Variable | Distrib. | Mean | CoV |
|----------------|----------|-----------------------|------|
| C_S | LN | 1 | 0.03 |
| C_{SIF} | LN | 1 | 0.07 |
| $\Delta\sigma$ | DET | | |
| A_a | LN | $4.80 \cdot 10^{-18}$ | 1.70 |
| A_b | LN | $5.86 \cdot 10^{-13}$ | 0.60 |
| m_a | DET | 5.10 | - |
| m_b | DET | 2.88 | - |
| K_{th} | LN | 140 | 0.4 |
| a_0 | LN | 0.15 | 0.66 |
| a_{cr} | DET | w/2 | - |

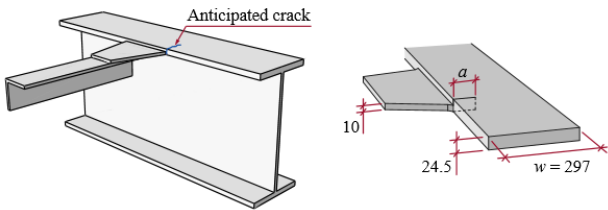


Figure 4: Dimensions and crack configurations of the gusset plate.

A crack is assumed to initiate and propagate into the flange at the end of a welded on in-plane gusset plate. For this detail, $Y(a)$ is defined by Newman Jr and Raju (1981) and $M_k(a)$ is given by Leander et al. (2013).

The stress range spectrum from gauge 101 is shown in Figure 5 and will be used for reliability assessment in the following section.

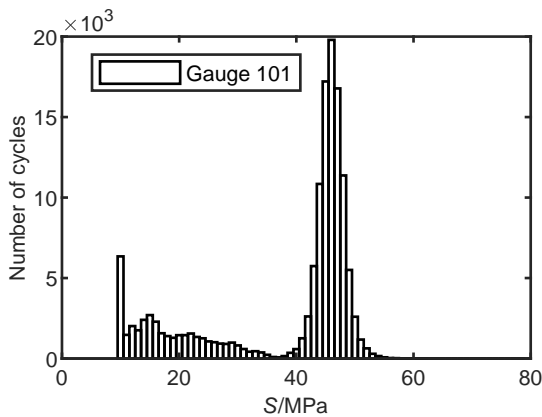


Figure 5: The stress range spectrum considered

4.1. Prior reliability assessment

MCS and SS with different settings are applied respectively to the detail in Figure 4 for its prior reliability assessment. Here the results are shown in Figure 6. The estimated fatigue life N_{cr} corresponding to $\beta = 3.1$ and the elapsed time are of interest and compared in Table 2.

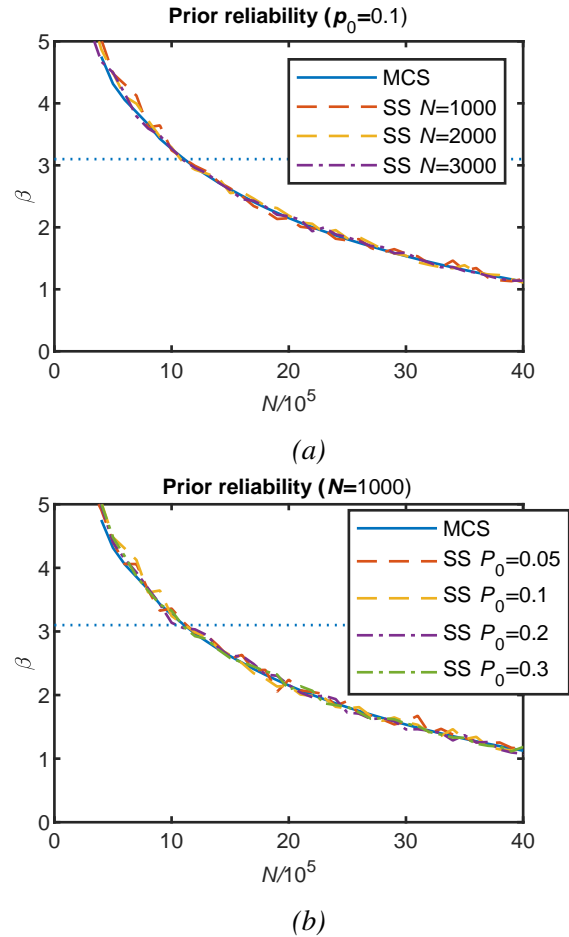


Figure 6: Performance of SS, for each subset iteration with: (a) different number of samples N ; (b) different conditional probability p_0

The fatigue life was estimated to 1.108 million cycles by MCS using one million samples, and it's regarded as the true value and compared with SS results as a reference.

The number of samples N for each subset iteration should be around one thousand or more to guarantee a consistent accuracy. Smaller than that will increase the randomness of the result. According to the last column in Table 2(a), N_{cr} are all within 5% deviation from MCS. However, the de-

Table 2: Estimated fatigue life corresponding to $\beta = 3.1$, for each subset iteration with (a) different number of samples N ; (b) different conditional probability p_0

| Simulation Method | Sample numbers | $N_{cr} / 10^5$ cycles | Elapsed time/h | Difference (compared to MCS) |
|-------------------|----------------|------------------------|----------------|------------------------------|
| MCS | 10^6 | 11.08 | 4.80 | - |
| SS ($p_0=0.1$) | 1000 | 11.10 | 0.82 | 0.18% |
| | 2000 | 10.77 | 1.62 | 2.79% |
| | 3000 | 10.91 | 2.38 | 1.53% |

(a)

| Simulation Method | Sample numbers | $N_{cr} / 10^5$ cycles | Elapsed time/h | Difference (compared to MCS) |
|-------------------|----------------|------------------------|----------------|------------------------------|
| MCS | 10^6 | 11.08 | 4.80 | - |
| SS | $p_0=0.05$ | 1000 | 11.28 | 1.80% |
| | $p_0=0.1$ | | 11.10 | 0.22% |
| | $p_0=0.2$ | | 11.55 | 4.24% |
| | $p_0=0.3$ | | 10.92 | 1.44% |

(b)

viations are not monotonically decreasing when N increases, which implies that using more samples doesn't necessarily reduce the deviation and improve the result, but certainly increases the elapsed time apparently. $N = 1000$ is the number of samples for one iteration. The total number of samples generated in the calculation would be the number of iterations multiply with N , and they are around 7 to 15 thousand depending on the value of $N_s(t)$, which are still far less than MCS.

The value of limit b_j for each subset adaptively corresponds to p_0 . A larger p_0 will induce a larger b_j , and more samples will be left as seeds to generate new samples for the next iteration. Then more iterations are required to approach the convergence and the calculation time will increase correspondingly. A too small p_0 increases the possibility that the simulation satisfies $b_j \leq 0$ at a very beginning stage and stops before reaching a converging result. In Table 2(b), four different values of p_0 were applied and the results didn't show much difference. Based on work from Au and Beck (2001), Schneider et al. (2017) and Li and Cao (2016), it is empirically reliable to use $p_0 = 0.1$ which is also confirmed by the results in Table 2(b).

Overall, the prior reliability assessments from SS are consistent with MCS as shown in Figure 6. And

the elapsed time for all settings are much shorter than MCS. It is apparent that SS shows better time efficiency in contrast to the high calculation cost of MCS. The feasibility of SS is proved to deal with a multi-dimensional LSF and a nonlinear crack propagation task.

4.2. Updated reliability assessment

An inspection with no detection was assumed when the prior reliability had decreased below $\beta = 3.1$, and an updated reliability assessment was performed. It is apparent in Figure 7 that considering inspection gives a significant increase in the fatigue life. The estimated fatigue lives corresponding to $\beta = 3.1$ are listed in Table 3.

The MCS result is the average value of 400 independent runs and is used as a reference to compare with SS. Three settings of SS with different number of samples N are applied and they showed consistent results. A similar phenomenon appears as the deviation exists and doesn't decrease monotonically when more samples are applied, which will be further explained by using a sensitivity analysis in Section 4.3. The results from updated reliability indicate that a beneficial influence on the fatigue life can be expected from inspection. And SS is feasible and works well in a reliability updating application.

Table 3: Updated fatigue life corresponding to $\beta = 3.1$

| Simulation Method | Sample number | $N_{cr}/10^5$ cycles | Elapsed time/h | Difference (compared to MCS) |
|--------------------|---------------|----------------------|----------------|------------------------------|
| MCS | 10^6 | 15.38 | - | - |
| SS ($p_0 = 0.1$) | 1000 | 15.19 | 0.55h | 1.23% |
| | 2000 | 15.25 | 0.98h | 0.84% |
| | 3000 | 15.88 | 1.65h | 3.25% |

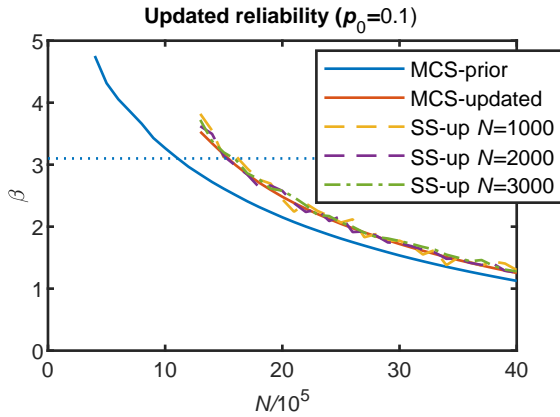


Figure 7: Updated reliability

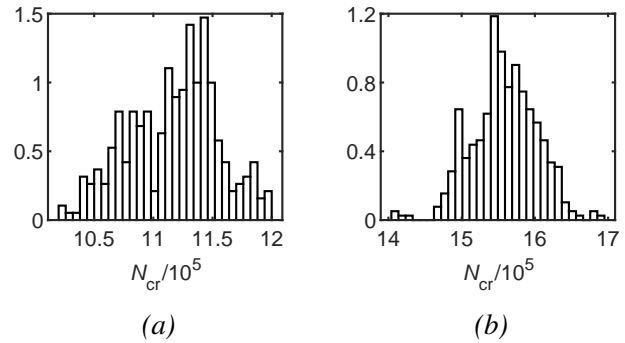


Figure 8: (a) Scattered prior fatigue life; (b) Scattered updated fatigue life corresponding to target $\beta = 3.1$ after 400 times independent simulation runs

4.3. Robustness of SS

According to the observations that a deviation always exists and doesn't have a regular pattern of variation, it is believed that the deviation exists due to inevitable randomness. A sensitivity test about the robustness of SS is tested by 400 independent simulation runs with $p_0 = 0.1$ and $N = 1000$ per subset iteration. Both prior and updated reliability analyses were performed. The empirical distributions of the estimated fatigue lives are plotted in Figure 8. Their mean value, standard deviation and 95% confidence interval are summarized in Table 4. Though it is apparent that the scatter of N_{cr} doesn't follow a normal distribution, the data are relatively centered with limited coefficient of variance (CoV), which proves that SS is robust in reliability assessment and that the accuracy of one single run is acceptable.

5. CONCLUSIONS

A probabilistic model for crack propagation has been outlined and applied on a gusset plate detail, which is representative for the Rautasjokk Bridge. The stress spectrum was obtained by a six-gauges

Table 4: Scattered result

| Condition | Mean | Std | 95% confidence interval |
|-----------|-------|------|-------------------------|
| Prior | 11.17 | 0.38 | [11.17 ± 0.63] |
| Updated | 15.58 | 0.44 | [15.58 ± 0.67] |

monitoring campaign. Both prior and updated reliability analyses have been performed by MCS and SS respectively. The following conclusions can be drawn:

- SS shows promising feasibility to deal with multi-dimensional LSFs and the crack propagation task with strong nonlinearity. By using MCS result obtained from one million samples as a reference, the SS routine obtains the consistent result by using limited number of iterations and one thousand samples for each iteration, which greatly reduces the calculation time. It proves that SS has a higher time efficiency compared to the high computation cost of MCS.
- The number of samples for each subset iter-

ation N can provide a good accuracy when it is around one thousand or higher. More samples than required can't eliminate the variance of the result but will consume more time. The conditional probability p_0 doesn't have much influence in this case and an empirical value $p_0 = 0.1$ is recommended.

- The robustness of SS was tested by 400 independent simulation runs both for prior and updated reliability estimation. The scattered estimated fatigue lives are relatively centered with limited CoV. It is believed that SS is robust and the result from one single simulation is acceptable and reliable.
- Visual inspection provided a noticeable increase in reliability and fatigue life.

The Rautasjokk Bridge has several fatigue prone details which can be regarded as a series system. A system reliability assessment would be of interest as a further study. Furthermore, a risk-based assessment of the bridge is expected by considering all possible failure scenarios. A framework is expected to be generalized from those outcomes.

6. REFERENCES

- Au, S. and Beck, J. (2003). "Important sampling in high dimensions." *Structural safety*, 25(2), 139–163.
- Au, S.-K. and Beck, J. L. (2001). "Estimation of small failure probabilities in high dimensions by subset simulation." *Probabilistic engineering mechanics*, 16(4), 263–277.
- Au, S.-K. and Wang, Y. (2014). *Engineering risk assessment with subset simulation*. John Wiley & Sons.
- BSI (2013). "Guide to methods for assessing the acceptability of flaws in metallic structures." *BS 7910:2013*.
- DNV GL (2015). "Probabilistic methods for planning of inspection for fatigue cracks in offshore structures. recommended practice." *Report No. DNVGL-RP-C210*, DNV GL AS.
- Guo, T. and Chen, Y.-W. (2013). "Fatigue reliability analysis of steel bridge details based on field-monitored data and linear elastic fracture mechanics." *Structure and Infrastructure Engineering*, 9(5), 496–505.
- Häggström, J. (2015). "Bärighetsberäkning: Bro över rautasjokk km 1432+883 (in Swedish)." *Luleå tekniska universitet*.
- Hobbacher, A. (1992). "Stress intensity factors of plates under tensile load with welded-on flat side gussets." *Engineering fracture mechanics*, 41(6), 897–905.
- Hohenbichler, M. and Rackwitz, R. (1981). "Non-normal dependent vectors in structural safety." *Journal of the Engineering Mechanics Division*, 107(6), 1227–1238.
- ISO 13822 (2010). "Bases for design of structures - assessment of existing structures.
- JCSS (2011). "Probabilistic model code." *Joint Committee on Structural Safety (JCSS)*.
- Leander, J., Andersson, A., and Karoumi, R. (2010). "Monitoring and enhanced fatigue evaluation of a steel railway bridge." *Engineering Structures*, 32(3), 854–863.
- Leander, J., Aygül, M., and Norlin, B. (2013). "Refined fatigue assessment of joints with welded in-plane attachments by lefm." *International Journal of Fatigue*, 56, 25–32.
- Li, H.-S. and Cao, Z.-J. (2016). "Matlab codes of subset simulation for reliability analysis and structural optimization." *Structural and Multidisciplinary Optimization*, 54(2), 391–410.
- Liu, M., Frangopol, D. M., and Kwon, K. (2010). "Fatigue reliability assessment of retrofitted steel bridges integrating monitored data." *Structural Safety*, 32(1), 77–89.
- Mooney, C. Z. (1997). *Monte carlo simulation*, Vol. 116. Sage Publications.
- Newman Jr, J. and Raju, I. (1981). "An empirical stress-intensity factor equation for the surface crack." *Engineering Fracture Mechanics*, 15(1-2), 185–192.
- Papaioannou, I., Betz, W., Zwirgmaier, K., and Straub, D. (2015). "MCMC algorithms for subset simulation." *Probabilistic Engineering Mechanics*, 41, 89–103.
- Paris, P. C. (1961). "A rational analytic theory of fatigue." *The Trend in Engineering*, 13, 9.
- Schneider, R., Thöns, S., and Straub, D. (2017). "Reliability analysis and updating of deteriorating systems with subset simulation." *Structural Safety*, 64, 20–36.
- Song, S., Lu, Z., and Qiao, H. (2009). "Subset simulation for structural reliability sensitivity analysis." *Reliability Engineering & System Safety*, 94(2), 658–665.
- Wang, F. and Li, H. (2017). "Subset simulation for non-gaussian dependent random variables given incomplete probability information." *Structural Safety*, 67, 105–115.